



DEGREE PROJECT IN ELECTRICAL ENGINEERING,
SECOND CYCLE, 30 CREDITS
STOCKHOLM, SWEDEN 2020

Comparison of LoRa and NB- IoT in Terms of Power Consumption

LUNTE TAN

Comparison of LoRa and NB-IoT in Terms of Power Consumption

Lunte Tan

Supervisor: Rong Du

Examiner: Carlo Fischione

Date: January 24, 2020

Abstract

The Low-Power Wide Area Network (LPWAN) offers longer transmission range and lower energy consumption. There are many LPWA technologies, such as Narrowband Internet of Things (NB-IoT) and Long Range (LoRa). These technologies are mainly battery-based and the energy consumption is an critical issue. There are few researches that focus on comparing the power consumption of LoRa and NB-IoT based on experiment results.

The objective of the thesis is to compare the power consumption of LoRa and NB-IoT. In this thesis, we did experiments to measure the power consumption of LoRa and NB-IoT. We calculated the estimated battery lifetime for different parameters based on our experiment results. The estimated battery lifetime shows that LoRa with SF7 has lower power consumption than NB-IoT.

Abstrakt

Low-Power Wide Area Network (LPWAN) erbjuder längre transmissionsintervall och lägre energiförbrukning. Det finns många LPWA-teknologier, till exempel Narrowband Internet of Things (NB-IoT) och Long Range (LoRa). Denna teknik är huvudsakligen batteribaserad och energiförbrukningen är en kritisk fråga. Det finns få undersökningar som fokuserar på att jämföra kraftförbrukningen av LoRa och NB-IoT baserat på experimentresultat.

Målet med avhandlingen är att jämföra kraftförbrukningen för LoRa och NB-IoT. I den här avhandlingen gjorde vi experiment för att mäta strömförbrukningen för LoRa och NB-IoT. Vi beräknade den beräknade batteritiden för olika parametrar baserat på våra experimentresultat. Den uppskattade batteritiden visar att LoRa med SF7 har lägre energiförbrukning än NB-IoT.

Acknowledgement

The radio module of LoRa is supported by Digital Nordix (DNX). The sim card for NB-IoT is supported by Telia. I would like to thank DNX and Telia for providing devices.

I would like to thank supervisor Rong Du and Professor Carlo Fischione for giving technical support and advice. I would like to express gratitude to Anders Carlberg from DNX for giving the technical support on LoRa-based programming.

I would like to thank Urban ICT Arena for providing testbeds. I would like to thank Mikael Prytz for providing an office room for my experiment.

I would like to thank Lu Jiang for setting up the environment for LoRa and NB-IoT communication together.

Contents

List of Figures	vi
List of Tables	vii
List of Acronyms	viii
1 Introduction	1
1.1 Low-Power Wide-Area Network	1
1.2 LoRa and LoRaWAN overview	2
1.3 NB-IoT overview	2
1.4 Thesis objective and contributions	3
1.5 Thesis structure	3
2 Preliminary	5
2.1 LoRa basics	5
2.1.1 Regional specification	5
2.1.2 Bit rate, spreading factor, code rate	5
2.1.3 Packet structure	6
2.1.4 Time on air	6
2.1.5 Duty cycle	7
2.1.6 Battery life/ Energy consumption	7
2.2 NB-IoT basics	8
2.2.1 Frequency band	8
2.2.2 Frame structure	8
2.2.3 Uplink transmission scheme	8
2.2.4 Data Rate	10
3 LoRa VS NB-IoT	11
3.1 Instruments	11
3.1.1 Technical specification	11
3.1.2 Structure of the design	13
3.2 Experiment process	13
3.3 Time interval	14
3.4 Measurement	15
3.5 Results	15

4	Analysis	18
4.1	Curve fitting	18
4.1.1	Fitting by piecewise linear function	18
4.1.2	Fitting by exponential function	21
4.2	Comparison	24
4.3	Performance of LoRa with different spreading factors	26
4.4	Performance of NB-IoT for different subcarrier spacing	28
4.5	Battery lifetime comparison	30
5	Conclusion	32
	References	34

List of Figures

1.1	LoRaWAN network topology	2
1.2	Network for the NB-IoT data transmission and reception	3
2.1	LoRa packet structure	7
2.2	Frame structure of NB-IoT	9
2.3	Resource grids for 15 kHz subcarrier spacing and 3.75 kHz subcarrier spacing of NB-IoT	9
2.4	Preamble symbol group	10
3.1	LoRa end device that is used in the experiments	13
3.2	NB-IoT end device that is used in the experiments	13
3.3	Data collection	14
3.4	MQTT server used in the experiments	14
3.5	The measurements of the battery voltage of the LoRa end device at different elapsed time.	17
3.6	The measurements of the battery voltage of the NB-IoT end device at different elapsed time.	17
4.1	Fitting linear piecewise function of the voltage from 4.2 V to 3.9 V for LoRa end device with the data of sample No. 5.	19
4.2	Fitting linear piecewise function of the voltage from 3.9 V to 3.7 V for LoRa end device with the data of sample No. 5.	19
4.3	The fitting linear piecewise function of the voltage from 4.2 V to 3.9 V for NB-IoT end device with the data of sample No. 6.	21
4.4	The fitting linear piecewise function of the voltage from 3.9 V to 3.7 V for NB-IoT end device with the data of sample No. 6.	21
4.5	The fitting exponential function of the voltage for LoRa end device with the data of sample No 5.	23
4.6	The fitting exponential function of the voltage for NB-IoT end device with the data of sample No 6.	23
4.7	ToA vs payload size for different spreading factors	26
4.8	Energy per useful bit vs payload size for different spreading factors. The payload size ranges from 0 to 1000 Bytes.	27
4.9	NPUSCH packet structure	28
4.10	Transmission time vs payload size with 1 repetition and 64 repetitions.	30
4.11	The energy per transmission as a function of payload size for SF7, SF12, and NB-IoT.	30

List of Tables

2.1	LoRaWAN regional specification	6
2.2	Parameters of default channels in EU868	6
2.3	NB-IoT frequency bands	8
2.4	Resource unit options for NPUSCH format 1 with 15 kHz spacing	10
3.1	Technical specification of Arduino MKR WAN 1300	12
3.2	Current consumption of the units in Arduino MKR WAN 1300	12
3.3	Technical specification of MKR NB 1500	12
3.4	Current consumption of the units in MKR NB 1500	12
3.5	Data rates of LoRaWAN under different configurations	15
3.6	A set of data for LoRa communication	16
4.1	The linear fitting result of the voltage as a function of time for the LoRa end device with the data we collected during the 5 trials.	19
4.2	The mean and standard deviation of the slope of the voltage transition functions for the LoRa end device with the data we collected during the 5 trials.	19
4.3	The linear fitting result of the voltage as a function of time for the NB-IoT end device with the data we collected during the 6 trials.	20
4.4	The mean and standard deviation of the slope of voltage transition functions for the NB-IoT end device with the data we collected during the 6 trials.	20
4.5	Mean values of R-square values for LoRa and NB-IoT with different constant values C	21
4.6	The exponential model fitting result of the voltage as a function of time for the LoRa end device with the data we collected during 5 trials.	22
4.7	The exponential model fitting result of the voltage as a function of time for the NB-IoT end device with the data we collected during 6 trials.	22
4.8	The mean values of the slope of the voltage transitions for Arduino boards without running codes	24
4.9	Energy per useful bit for different spreading factors (Payload size=1000 Bytes)	27
4.10	SX1276 characteristics	28
4.11	Calculated header length for different options	29
4.12	Estimated battery lifetime.	31

List of Acronyms

CIoT	Cellular Internet of Things
DMRS	Demodulation Reference Signal
EPS	Evolved Packet System
IoT	Internet of Things
LoRa	Long Range
LPWAN	Low-Power Wide-Area Network
MCL	Maximum Coupling Loss
NB-IoT	Narrowband Internet of Things
NPRACH	Narrowband Physical Random Access Channel
NPUSCH	Narrowband Physical Uplink Shared Channel
OFDM	Orthogonal Frequency-Division Multiplexing
SC-FMDA	Single-Carrier Frequency-Division Multiple Access
TBS	Transport Block Size
ToA	Time on Air

Chapter 1

Introduction

Ericsson illustrates the Network Society vision in its white paper: "where everything that benefits from a connection is connected" [1]. The Internet of Things (IoT) expresses this vision and revolutionizes our lifestyle. The applications of IoT, which include smart city, smart vehicles, and smart agriculture, are affecting our entire ecosystem. These applications help us improve the efficiency of working and living, environmental protection, and energy saving. IoT brings the wave of communication revolution and is growing rapidly. According to Ericsson Mobility Report [2], the world will have 29 billion connected devices by 2022 and 18 billion of them will be IoT-related.

As the growth of the IoT, more new requirements on the IoT appear such that those new applications would be fulfilled. For example, to enable the monitoring of large area for multiple years without the need of battery changing, the need of long transmitting distance and low power consumption shows up. The solutions such as Bluetooth, ZigBee, and WLAN no longer fit this scenario. Low-Power Wide-Area Networks (LPWANs) are the appropriate solutions for such situations.

1.1 Low-Power Wide-Area Network

LPWAN is the name for all low-power network technologies in wide area. These wireless communications can either use licensed bands or unlicensed bands. LPWANs offer better power efficiency, lower cost, and longer transmission range. To enable these advantages, LPWAN technologies have a low data rate, which is typically up till 50 kbit/s. For the scenarios that are delay tolerant, LPWANs can provide a device with a coverage of several kilometers and a long-life cycle of several years. To sum up, the major advantages of LPWANs are easy deployment, low cost (devices and deployment), great power efficiency, security, and long coverage for communication. These make LPWA technologies much more crucial in smart building, smart city, industry, etc. Therefore, LPWA technologies show a great potential in economy and technology in the near future [3].

There are various LPWA technologies, such as SigFox, LoRa, LTE-M, and NB-IoT. LoRa and NB-IoT are two mainstream LPWA technologies which stands for unlicensed spectrum options (LoRa and SigFox) and licensed spectrum options (NB-IoT and LTE-M). The following parts bring the brief overview

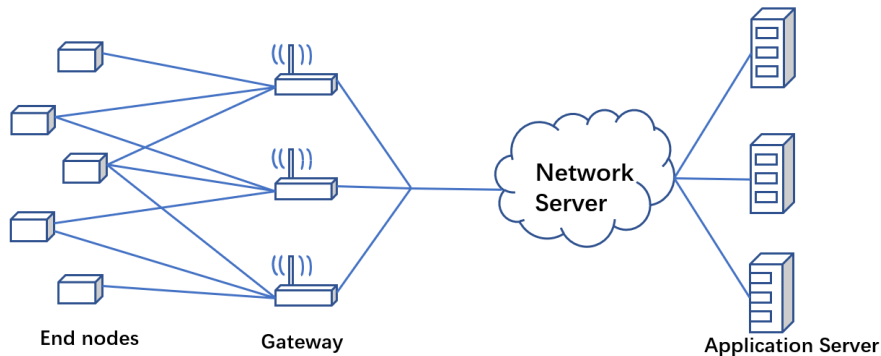


Figure 1.1: LoRaWAN network topology

of LoRa and NB-IoT.

1.2 LoRa and LoRaWAN overview

There is a need to distinguish two different terminologies: LoRa and LoRaWAN.

LoRa is the wireless modulation or the physical layer for the LPWANs to enable the long-range communications [4]. LoRa is based on the Chirp-spread-spectrum (CSS) modulation so that it can maintain low power characteristics when the increasing communication range is ensured [9].

Since LoRa is the physical layer protocol, the upper layers need protocols. LoRaWAN is the communication protocol that manages communications between end nodes and gateway [4]. The network topology of LoRaWAN is shown in Figure 1.1. LoRaWAN network uses a star-of-star topology where gateways relay the messages between end nodes and a central network server [5]. LoRaWAN supports bidirectional communications between end node and gateway.

The network topology of LoRaWAN influences on battery lifetime, the network capacity, and the network applications. Meshed network architecture is widely used in existing networks, but it will reduce battery lifetime and bring more redundant information if the communication range increases [4]. On the other hand, the end nodes are connected to central connection point in star topology, so there is less redundant information when the communication range increases. Therefore, compared to mesh network, long range star architecture is the better choice for preserving batter lifetime when achieving the long-range communication [4].

1.3 NB-IoT overview

NB-IoT is a LPWA technology standardized in 3GPP Release 13 to enable long coverage and low power consumption [6]. NB-IoT is specified to compete with non-3GPP technologies and optimizes the support by cellular networks.

NB-IoT reuses many designs of the LTE physical layers and higher layers to save the time for product development, such as downlink orthogonal frequency-

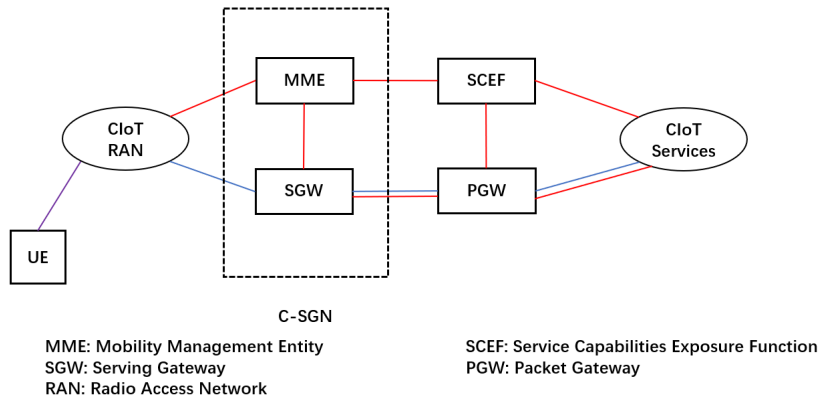


Figure 1.2: Network for the NB-IoT data transmission and reception. In red, the control plane optimization for the cellular internet of things in the evolved packet system is indicated. In blue, the user plane optimization for the cellular internet of things in the evolved packet system is indicated [8].

division multiple access (DL OFDM), uplink single-carrier frequency-division multiple access (UL SC-FMDA), channel coding, rate matching, etc [7]. Many advanced LTE features are greatly simplified in order to reduce power consumption.

Two optimizations for the cellular Internet of Things (ClIoT) in the evolved packet system (EPS) were specified to optimize the data transmission. These are the User Plane ClIoT EPS optimization and the Control Plane ClIoT EPS optimization, as shown in Figure 1.2. The correct choice for the optimizations could reduce signaling and save more power consumption [7].

1.4 Thesis objective and contributions

As introduced in the previous section, power efficiency and low cost are the advantages of the LPWANs. Most applications are based on battery and the energy consumption decides the lifetime of them. For most scenarios, such as smart agriculture and smart building, we prefer long duration of the devices. It is critical to investigate the characteristic of the energy consumption.

In this degree project, we will conduct some experiments to compare the energy consumption of the LoRaWAN and NB-IoT. Based on our measurements, we calculate the power consumption of the LoRa transmission and NB-IoT transmission. In analysis, we calculate the estimated battery lifetime for LoRa and NB-IoT with different parameters.

1.5 Thesis structure

The rest of the thesis is organized as follows. In Chapter 2, some basic concepts of LoRa and NB-IoT will be introduced. The experiment setup and the results will be shown in Chapter 3. Chapter 4 presents the analysis based on the

experimental results, and the comparison of NB-IoT and LoRa in terms of power consumption. Chapter 5 concludes the experiments, and discusses some potential future work.

Chapter 2

Preliminary

In this part, some basic concepts of LoRa and NB-IoT are demonstrated. The first section presents the regional specification and some parameters of LoRa which are related to the transmission. The second section shows the frequency band of NB-IoT and the uplink transmission scheme.

2.1 LoRa basics

2.1.1 Regional specification

The LoRaWAN has different specifications in each region based on the regional spectrum allocations [4]. In this project, we focus on the specification on Europe, as shown in Table 2.1.

In Europe, the regional parameter common name is EU868. There are three following default channels that must be implemented in every end-device for EU868 and all network gateways belongs to EU868 should always be listening on [10]. Their frequencies are 868.1 MHz, 868.3 MHz, and 868.5 MHz (Other parameters are shown in Table 2.2.)

2.1.2 Bit rate, spreading factor, code rate

In this subsection, we will introduce several configuration parameters for the LoRa radio, such as bandwidth (BW), spreading factor (SF), and code rate (CR) [12].

- **Bandwidth:** Bandwidth is the range of frequencies in the transmission and it is interchangeably with chip rate. Mostly 125 kHz is chosen. We denote it by BW .
- **Spreading factor:** Spreading factor is the number of raw bits that can be encoded by the symbol. It is denoted by SF . The signal can be divided into 2^{SF} chips. When the spreading factor is increased by 1, it takes double time on air to transmit the same data. Spreading factor is an integer and its range is 7 to 12.

	Europe	North America
Frequency band	867-869 MHz	902-928 MHz
Channels	10	64+8+8
Channel BW Up	125/250kHz	125/500kHz
Channel BW Dn	125kHz	500kHz
TX Power Up	+14 dBm	+20 dBm typ
TX Power Dn	+14 dBm	+27 dBm
SF Up	7-12	7-10
Data rate	250 bps-50 kbps	980 bps-21.9 kbps
Link Budget Up	155 dB	154 dB
Link Budget Dn	155 dB	157 dB

Table 2.1: LoRaWAN regional specification [4]

Modulation	LoRa
Bandwidth[kHz]	125
LoRa DR/Bitrate	DR0 to DR5/0.3-5 kbps
Nb Channels	3
Duty Cycle	< 1%

Table 2.2: Parameters of default channels in EU868[10]

- Coding rate: Coding rate is the proportion of the useful bits that carry information. We denote it by CR . The notation is:

$$CR = \frac{4}{CR + 4}, \quad (2.1)$$

where $n=1, 2, 3, 4$ in LoRa modulation.

Now, according to [11], we are ready to calculate the bit rate given those parameters as

$$R_b = SF \cdot \frac{BW}{2^{SF}} \cdot CR. \quad (2.2)$$

Using this equation, we can calculate the data rates for all spreading factors.

2.1.3 Packet structure

The LoRa packet structure is shown in Figure 2.1 [14]. It contains a preamble, an optional header, the payload and a cyclic Redundancy Check (CRC). The maximum size is between 51 Bytes and 222 Bytes, which depends on the SF.

2.1.4 Time on air

Time on air (ToA) is the transmission time of a LoRa packet. The calculation of ToA needs the combination of spreading factor, bandwidth, coding rate and



Figure 2.1: LoRa packet structure

the packet structure. ToA is the sum of the preamble duration and the payload duration, which is

$$ToA = T_{\text{preamble}} + T_{\text{payload}}, \quad (2.3)$$

where T_{preamble} is the preamble duration and T_{payload} is the payload duration. The preamble duration is calculated as

$$T_{\text{preamble}} = (n_{\text{preamble}} + 4.25)T_{\text{symbol}}, \quad (2.4)$$

where n_{preamble} is 8 symbols according to EU868.

The payload duration depends on the header mode and the low data rate optimization. The formula is given as follows [14]:

$$T_{\text{payload}} = T_{\text{symbol}} \left(8 + \max \left(\text{ceil} \left[\frac{8PL - 4SF + 44 - 20IH}{4(SF - 2DE)} \right] (CR + 4), 0 \right) \right), \quad (2.5)$$

where PL represents the payload size in Bytes. IH is the indicator of whether header is enabled ($IH = 0$, otherwise $IH = 1$). DE is the indicator of whether the LowDataRateOptimize is enabled ($DE = 1$, otherwise $DE = 0$).

The time for transmit a symbol (T_s) is based on the spreading factor and bandwidth:

$$T_s = \frac{2^{SF}}{BW}. \quad (2.6)$$

Combining Eq (2.4), Eq (2.5), and Eq (2.6), we can calculate the ToA based on the spreading factor and payload size.

2.1.5 Duty cycle

Duty cycle is the proportion of time that the device is busy. We denote transmission time by t and duty cycle by D . We can calculate the duty cycle as

$$D = \frac{ToA}{t}. \quad (2.7)$$

In Table 2.2, the regional specification is shown. The maximum duty cycle in EU868 is 1%. With such a constraint, it is necessary for enforcement pause between two transmissions.

2.1.6 Battery life/ Energy consumption

LoRaWAN network uses asynchronous and ALOHA-based protocol so the nodes can communicate whenever the message is ready. The nodes in LoRaWAN do

Band No.	UL frequency range (MHz)	DL frequency range (MHz)
1	1920 - 1980	2110 - 2170
2	1850 - 1910	1930 - 1990
3	1710 - 1785	1805 - 1880
5	824 - 849	869 - 894
8	880 - 915	925 - 960
12	699 - 716	729 - 746
13	777 - 787	746 - 756
17	704 - 716	734 - 746
18	815 - 830	860 - 875
19	830 - 845	875 - 890
20	832 - 862	791 - 821
26	814 - 849	859 - 894
28	703 - 748	758 - 803
66	1710 - 1780	2110 - 2200

Table 2.3: NB-IoT frequency bands

not need to synchronize and check for message compared to the synchronous network. The process of synchronization is a major part of consuming energy and reducing battery lifetime. In a study done by GSMA [4], LoRaWAN had a 3 to 5 times advantage compared to other technologies in the LPWAN space.

The parameters of LoRa modulation also have influence on the energy consumption. The increase of spreading factor will consume more energy for transmitting the same amount of data [12]. The increase of the spreading factor will increase the transmission range and the maximum payload at the same time. There is a trade-off between power consumption and transmission range when selecting the proper spreading factor.

2.2 NB-IoT basics

2.2.1 Frequency band

For frequency bands, the subset of the same frequency numbers in LTE is used, which is defined for NB-IoT. The frequency bands in Release 13 are shown in Table 2.3 [16]. Telia uses 3 LTE bands, which are Band 3, Band 7, and Band 20 [17].

2.2.2 Frame structure

For 15 kHz subcarrier spacing, the radio frame is divided into 10 subframes, each of which is composed of two slots. For 3.75 kHz sub-carrier spacing, each frame is directly divided into five slots. The radio frame is 10 ms duration. The structure is shown in Figure 2.2.

2.2.3 Uplink transmission scheme

NB-IoT supports single-tone and multi-tone transmissions for uplink transmission scheme. Multi-tone transmission applies the Single Carrier Frequency Di-

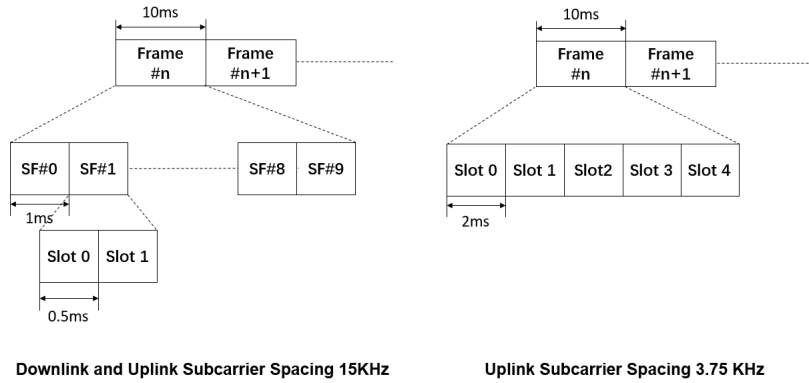


Figure 2.2: Frame structure of NB-IoT

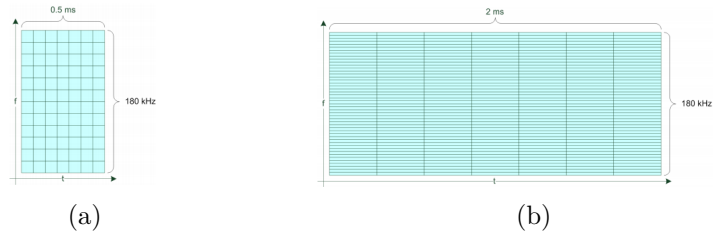


Figure 2.3: (a)Resource grid for 15 kHz subcarrier spacing. (b) Resource grid for 3.75 kHz subcarrier spacing [8]

vision Multiple Access (SC-FDMA) with a 15 kHz subcarrier spacing, 0.5 ms slot, and 1 ms subframe. Single-tone transmission supports both 3.75 kHz and 15 kHz subcarrier spacing. The 15 kHz numerology is similar to LTE. On the other hand, the symbol duration of the 3.75 kHz subcarrier uses a slot length of 2 ms because the time for 3.75 kHz subcarrier spacing is four times as the 15 kHz subcarrier spacing. Each slot consists of 7 OFDM symbols and the uplink subcarrier operates on a system bandwidth of 180 kHz. The resource grids of the slots for 15 kHz and 3.75 kHz have the structures shown in Figure 2.3.

The uplink of NB-IoT has two physical channels:

- Narrowband Physical Uplink Shared Channel (NPUSCH): NPUSCH has two defined formats. Format 1 serves as transmitting the uplink data over the uplink shared channel and uses turbo code for error correction. The maximum transport block size (TBS) is 1000 bits. Format 2 carries uplink control information and is used for the acknowledgement of a downlink transmission.

The modulation scheme is always BPSK for NPUSCH format 2 and uses BPSK or QPSK for single-tone transmission and always BPSK for other circumstances for NPUSCH format 1.

Resource unit (RU) is the smallest transport which is defined based on the frequency range (subcarrier) and time range (slot).

Number of subcarriers	Number of slots	RU Duration
1	16	8 ms
3	8	4 ms
6	4	2 ms
12	2	1 ms

Table 2.4: Resource unit options for NPUSCH format 1 with 15 kHz spacing



Figure 2.4: Preamble symbol group[8]

For NPUSCH format 1, an RU consists of 1 subcarrier with a length of 16 slots for 3.75 kHz subcarrier spacing and there are 4 options for 15 kHz spacing, as shown in Table 2.4 [8].

For NPUSCH format 2, an RU consists of 1 subcarrier with a length of 4 slots for both cases.

- Narrowband Physical Random Access Channel (NPRACH): A preamble is transmitted in the NPRACH. The preamble has 4 symbol groups, each of which has a cyclic prefix and five symbols as shown in Figure 2.4.

The preamble has two formats with different cyclic prefix (CP) lengths. The symbol duration of CP is $67 \mu\text{s}$ for format 0 and $267 \mu\text{s}$ for format 1. The duration of the five symbols in the preamble is 1.333 ms. A NPRACH preamble should be repeated 1, 2, 4, ..., 64 or 128 times depending on the coverage.

The uplink of NB-IoT has one physical signal:

- Demodulation Reference Signal (DMRS): DMRS is multiplexed with data, which means it is transmitted in the same RUs for the data transmission. The length of DMRS in one slot is either one or three SC-FDMA symbols.

2.2.4 Data Rate

For NPUSCH, the peak data rate is achieved by using largest TBS of 1000 bits in 4ms [18]. The peak data rate can reach 250kbps theoretically. However, it is lower in reality when considering the time offset. The sustained peak data rate is 62.5kbps.

Chapter 3

LoRa VS NB-IoT

This thesis aims at comparing the energy consumption of LoRa and NB-IoT based on experiments. In this part, we explain how we conducted the experiments to collect the data for analysis.

3.1 Instruments

In our experiments, we used two Arduino boards (MKR WAN 1300 for LoRa communication and MKR NB 1500 for NB-IoT communication), two 3.8 V Li-Po batteries, and two antennas with central frequency 868 MHz. To enable the NB-IoT communication, we chose Telia SIM card. For LoRa communication, the gateway from DNX was used. We used the application EUI and the application key for connections.

3.1.1 Technical specification

In this part, the technical specifications of the two Arduino boards are given. The values of the current consumption will be used in the analysis and discussion.

3.1.1.1 Arduino board for LoRa

Arduino MKR WAN 1300 can be powered by using Vin pin with a regulated 5 V source. The technical specification of Arduino MKR WAN 1300 is shown in Table 3.1 [19]. MKR WAN 1300 uses SAMD21 Cortex-M0+32bit low power ARM MCU as the microcontroller and uses CMWX1ZZABZ as the radio module. CMWX1ZZABZ is a module that comprises wireless transceiver Semtech SX1276 and an STMicro STM32L0 series ARM Cortex-M0+ 32 bit microcontroller (MCU).

The current consumption of the microcontroller and the radio module in standby mode is shown in Table 3.2 [20][21]. In standby mode, the current consumption of CMWX1ZZAB is 1.4 μ A. In idle mode, the current consumption of CMWX1ZZAB is 21.5 mA. SAM D21 consumes 4.06 mA in standby mode.

Note: The protocol stack of wireless radio module only includes 3GPP Release 13. The features of Release 14 and 15 are not enabled.

Microcontroller	SAMD21 Cortex-M0 +32bit low power ARM MCU
Radio module	CMWX1ZZABZ
Board Power Supply (USB/VIN)	5 V
Circuit Operating Voltage	3.3 V

Table 3.1: Technical specification of Arduino MKR WAN 1300

	Description	Typical	Max	Unit
CMWX1ZZABZ	STM32L0 in Standby mode SX1276 in Sleep mode	1.40		μA
CMWX1ZZABZ	Supply current in idle mode	21.5		mA
SAM D21	XOSC32K (Standby)	4.06	12.8	μA

Table 3.2: Current consumption of the units in Arduino MKR WAN 1300

Microcontroller	SAMD21 Cortex-M0 +32bit low power ARM MCU
Security	ECC 508 crypto chip
Wireless radio	UBLOX SARA-R410M-02B
Board Power Supply (USB/VIN)	5V
Circuit Operating Voltage	3.3V

Table 3.3: Technical specification of MKR NB 1500

Unit	Description	Typical	Max	Unit
ATECC508A	Operating Current Typical (mA)	1		mA
SARA-R4	PSM Deep Sleep Mode	8		μA
SARA-R4	Active Mode		9	mA
SARA-R4	LTE Cat NB1 Connected Mode (Avg)	130	240	mA
SARA-R4	LTE Cat NB1 Connected Mode (Peak)		0.5	A
SAM D21	XOSC32K (Standby)	4.06	12.8	μA

Table 3.4: Current consumption of the units in MKR NB 1500

3.1.1.2 Arduino board for NB-IoT

Arduino MKR NB 1500 can be powered by using Vin pin with a regulated 5 V source. The technical specification of Arduino MKR NB 1500 is in Table 3.3 [22]. MKR NB 1500 uses ECC 508 crypto chip for security and SARA-R4 for wireless radio.

The current consumption of the given units are shown in Table 3.4 [21][23]. SARA-R4 consumes 8 μA in power saving mode and 9 mA in active mode. In connected mode for NB-IoT transmission, the current consumption of SARA-R4 is 130 mA in average.

From Tables 3.2 and 3.4, we can see the radio module for LoRa consumes less power in deep sleep mode.

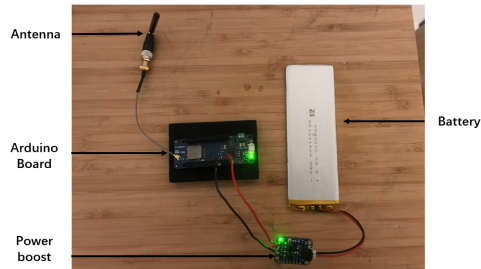


Figure 3.1: LoRa end device that is used in the experiments

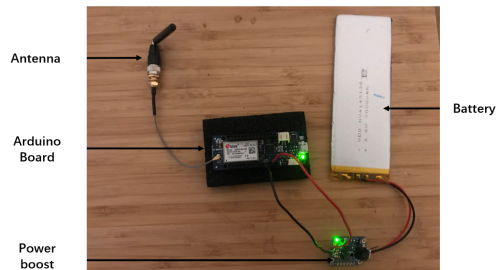


Figure 3.2: NB-IoT end device that is used in the experiments

3.1.2 Structure of the design

The structure of the design is presented in Figure 3.1 and Figure 3.2. The battery we used is 3.8 V Li-Po battery and both boards require 5 V input voltage for their Vin pin. Here we used the same power boost to provide steady 5 V input voltage. Both Arduino boards used the same type of antenna.

3.2 Experiment process

These two Arduino boards can serve as the end devices of LoRa and NB-IoT communications. The whole transmission is shown in Figure 3.3. In our experiments, the end devices will transmit message consecutively. After passing the gateway, the data will be sent to the network sever. We need to collect the data to check whether the communication is successful. In our experiments, the data was collected from the MQTT server.

MQTT server is used for the message receiving. We used a software, MQTT-Box, to check the data sent to the MQTT server. With a certain topic and broker address, the related message is shown. For NB-IoT, we chose "broker.hivemq.com" as the broker. For LoRaWAN, we used the DNX gateways for communication. The one for LoRaWAN is mqtt.digitalnordix.com which is provided by DNX.

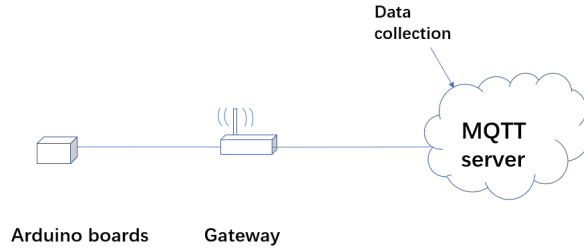


Figure 3.3: Data collection

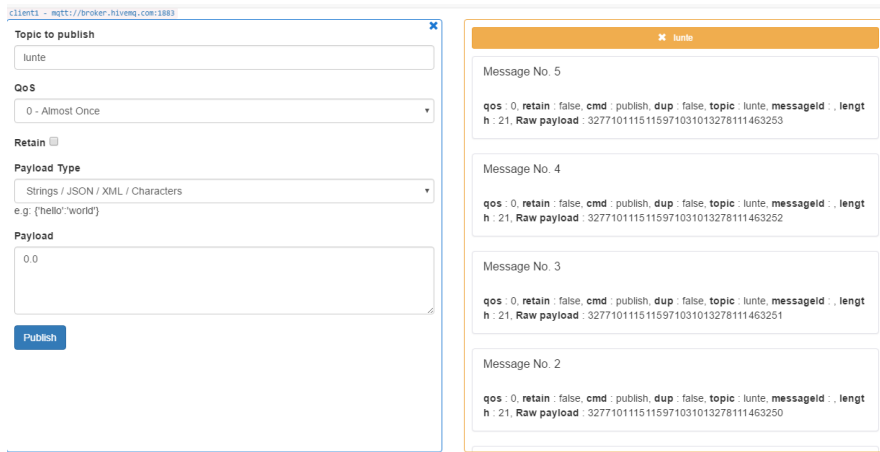


Figure 3.4: MQTT server used in the experiments

3.3 Time interval

Since the energy consumption of LPWANs is very low, the time interval between the transmissions should be small so that the change of battery voltage can be noticeable for measurements. In this section, we aim at choosing a proper time interval.

Due to the constraint of the duty cycle, LoRa needs to wait a certain time for next transmission. The minimum time interval is based on the chosen data rates. The data rates of LoRaWAN in Europe are shown in Table 3.5. From the table, we can see the bit rates differ from 250 bits/s to 5470 bits/s, which makes the minimum time interval different. As introduced in Section 2.1.5, the maximum duty cycle is 1%. To select the shortest time interval, we choose the smallest spreading factor: 7. The time interval is calculated as

$$T_{\text{interval}} = \frac{ToA}{D}. \quad (3.1)$$

The payload we used in the experiment is 50 Bytes. With Eq (2.3), Eq (2.4),

Data Rate	Configuration	bits/s	Max payload
DR0	SF12/125 kHz	250	59
DR1	SF11/125 kHz	440	59
DR2	SF10/125 kHz	980	59
DR3	SF9/125 kHz	1760	123
DR4	SF8/125 kHz	3125	230
DR5	SF7/125 kHz	5470	230

Table 3.5: Data rate of LoRaWAN under different configurations [24]

and Eq (2.5), the ToA is calculated.

For a payload with 50 Bytes, the ToA for SF7/125 kHz is 97.54 ms. Thus, the shortest time interval is around 10 s for this case. To make the comparison fair, we set the time interval for sending consecutive message as 10 s in both Arduino boards.

3.4 Measurement

To measure the power consumption of LoRa and NB-IoT, we needed to measure the transition of the battery power with the elapse of time. Since we did not have the method to measure the battery power directly, we chose to measure the voltage change for comparison to estimate the change of the battery power. The battery is charged to around 4.17 V and we kept measuring the voltage change until the battery cannot support transmission. The voltage data is measured every 45-90 minutes when the voltage is above 3.6 V. When the voltage is lower than a certain level, the voltage changes dramatically. The time interval for measuring low voltage changes to 30 minutes.

The end devices (Arduino boards) were placed in Kista, where the network coverage of LoRa and NB-IoT is good and the retransmission due to the packet loss is not a concern. During the measurements, the devices were switched off at night since measuring process was unavailable at night and restarted in the morning.

Battery capacity may drop due to the charging and discharging. The dropping of the same type of battery may differ. For example, a battery capacity may drop faster while the other one does not drop much. To minimize such a difference, two end devices take turns to use two batteries.

3.5 Results

To visualize the result, we plot voltage vs time of each sample. During the measurement, we paused at night and started in the morning. Here we consider that this process has no influence and only consider time interval as the variable.

The corresponding data for LoRa communication is shown in Table 3.6. In the table, we can see the measurement is paused several times. It took 3502 minutes for consuming all the energy in this case. In total, we measure 5 datasets for LoRa and 6 datasets for NB-IoT.

Date	Real time	Voltage (V)	Time (min)
2019/10/9	9:07	4.1	0
	10:07	4.08	60
	10:54	4.08	107
	12:56	4.06	229
	14:22	4.04	315
	16:05	4.01 (Pause)	418
2019/10/10	10:28	Start	
	11:53	3.98	503
	12:28	3.972	538
	13:28	3.965	598
	14:33	3.948	663
	15:38	3.931	728
	16:24	3.92	774
	17:29	3.908 (Pause)	839
2019/10/11	10:11	Start	
	11:19	3.897	907
	11:50	3.893	938
	12:39	3.886	987
	13:30	3.878	1038
	14:45	3.865	1113
	15:54	3.857	1182
	16:48	3.85	1236
	10:24	3.749	2292
	11:09	3.745	2337
	12:46	3.739	2434
	13:18	3.736	2466
	14:14	3.731	2522
	15:05	3.725	2573
	16:00	3.717	2628
	7:07	3.705 (Pause)	2695
2019/10/12	12:00	Start	
	13:42	3.684	2797
	14:34	3.675	2849
	15:53	3.67	2928
	16:53	3.669 (Pause)	2988
2019/10/13	11:09	Start	
	12:03	3.665	3042
	13:16	3.66	3115
	14:16	3.656	3175
	14:51	3.645	3210
	15:13	3.629	3242
	15:36	3.606	3265
	15:49	3.59	3278
	15:59	3.578	3288
	16:22	3.547	3311
	16:38	3.523	3327
	19:33	End	3502

Table 3.6: A set of data for LoRa communication

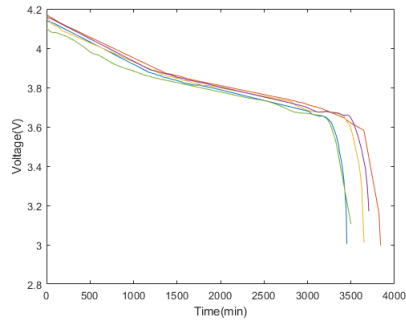


Figure 3.5: The measurements of the battery voltage of the LoRa end device at different elapsed time. The lines with different colors represent the results of different trials. All the trials are measured from fully charged to empty.

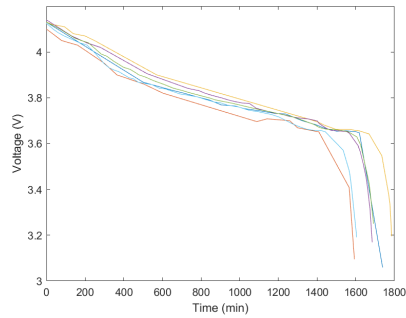


Figure 3.6: The measurements of the battery voltage of the NB-IoT end device at different elapsed time. The lines with different colors represent the results of different trials. All the trials are measured from fully charged to empty.

The corresponding figures for LoRa end device and NB-IoT end device based on the collected data during several trials are shown in Figure 3.5 and Figure 3.6. We can see that there is a sharp transition when the voltage is relatively low (below 3.65 V). The transition from 4.2 V to 3.7 V seems to be piecewise linear. From Figure 3.5, we can see there is a turning point at around 3.9 V.

Chapter 4

Analysis

In this part, we analyze the collected data from Chapter 3 and calculate the energy consumption of LoRa and NB-IoT.

4.1 Curve fitting

Based on the voltage data we collected, as we have presented in Figure 3.5 and Figure 3.6, there is a sharp transition when the voltage is relatively low (below 3.65 V). In our experiments, we decide to discuss the result excluding that part. To fit the result with curves, we use fitting by piecewise linear function and fitting by exponential function.

4.1.1 Fitting by piecewise linear function

From Figure 3.5 and Figure 3.6, we can see there is a turning point at around 3.9V. Then we can classify the curve as the combination of two linear curves:

$$V_1(t) = p_1t + C_1 \quad (3.9V \leq V \leq 4.2 \text{ V}),$$

$$V_2(t) = p_2t + C_2 \quad (3.7V \leq V \leq 3.9 \text{ V}).$$

In the following part, we use this model to fit the curves for LoRa and NB-IoT.

4.1.1.1 LoRa

Based on the data on Figure 3.5, we calculate the corresponding slope of each data set by `cftool` in Matlab, as shown in Table 4.1. We can see the R-square of each data is close to 1, which shows that the data fits the linear model well.

The mean and standard deviation of these 5 data sets are shown in Table 4.2. We can see the slope data of linear fitting do not vary much and the slope for 3.9 V to 3.65 V is more precise when comparing the standard deviation.

To visualize whether data fit the linear well, we present one sample as an example. In Table 4.1, every sample shows similar R-square, so we take sample 5 as an example. The parameters of both fitting curves are shown in Figure 4.1 and Figure 4.2. We can see that all the data points are close to the fitting linear function, which implies the transition of the voltage fits well with the line. We conclude that linear fitting is a plausible solution for the data.

set #	Slope 4.2 V to 3.9 V	R-square	Slope 3.9 V to 3.7 V	R-square
1	-0.0002254	0.997	-0.0001050	0.994
2	-0.0002141	0.990	-0.0001039	0.981
3	-0.0002072	0.989	-0.0001032	0.994
4	-0.0002272	0.999	-0.0001040	0.999
5	-0.0002325	0.993	-0.0001027	0.995

Table 4.1: The linear fitting result of the voltage as a function of time for the LoRa end device with the data we collected during the 5 trials.

	mean	standard deviation
4.2 V to 3.9 V	-2.2128e-04	1.0330e-05
3.9 V to 3.7 V	-1.0377e-04	8.9215e-07

Table 4.2: The mean and standard deviation of the slope of the voltage transition functions for the LoRa end device with the data we collected during the 5 trials.

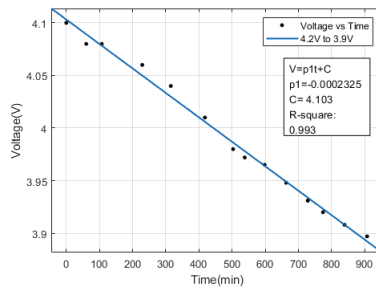


Figure 4.1: Fitting linear piecewise function of the voltage from 4.2 V to 3.9 V for LoRa end device with the data of sample No. 5.

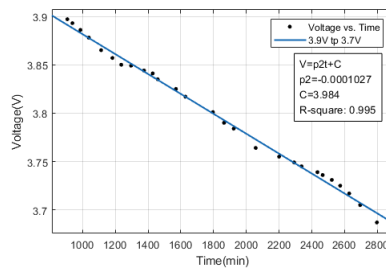


Figure 4.2: Fitting linear piecewise function of the voltage from 3.9 V to 3.7 V for LoRa end device with the data of sample No. 5.

set #	Slope	R-square	Slope	R-square
	4.2 V to 3.9 V		3.9 V to 3.7 V	
1	-0.0005246	0.991	-0.0001933	0.978
2	-0.0005225	0.981	-0.0002347	0.975
3	-0.0004407	0.985	-0.0002343	0.988
4	-0.0004354	0.981	-0.0002209	0.992
5	-0.0004904	0.996	-0.0002223	0.987
6	-0.0005622	0.984	-0.0002220	0.989

Table 4.3: The linear fitting result of the voltage as a function of time for the NB-IoT end device with the data we collected during the 6 trials.

	mean	standard deviation
4.2 V to 3.9 V	-4.9586e-04	5.0277e-05
3.9 V to 3.7 V	-2.2124e-04	1.5082e-05

Table 4.4: The mean and standard deviation of the slope of voltage transition functions for the NB-IoT end device with the data we collected during the 6 trials.

4.1.1.2 NB-IoT

Based on the data in Figure 3.6, the corresponding slope of either fitting line is calculated, as shown in Table 4.3. We can see the R-square of each slope is close to 1, which shows that the linear fitting is well.

The mean and standard deviation of each slope shown in Table 4.4. We can see that the standard deviation for both parts are small, which shows that the measurement is precise.

To visualize whether data fits the linear well, we take sample 6 as example. Since the R-square for every sample shows great performance, it makes no difference which sample is presented.

The parameters of both fitting curves are shown in Figure 4.3 and Figure 4.4. For the data for power consumption of the NB-IoT communication, the linear model shows good precision and accuracy. We conclude that the linear model is a plausible choice for our future analysis.

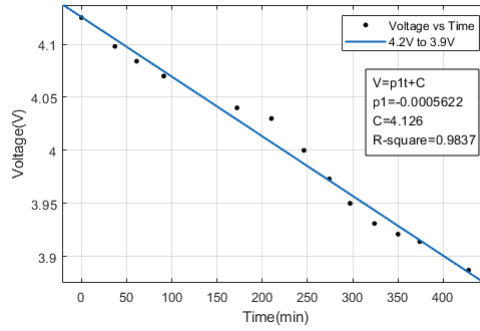


Figure 4.3: The fitting linear piecewise function of the voltage from 4.2 V to 3.9 V for NB-IoT end device with the data of sample No. 6.

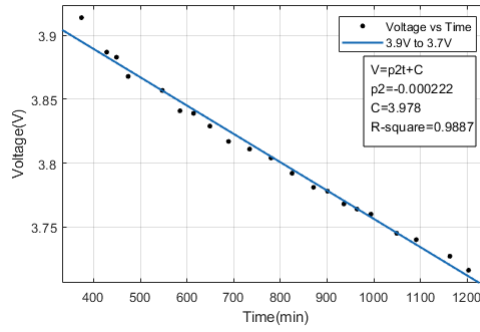


Figure 4.4: The fitting linear piecewise function of the voltage from 3.9 V to 3.7 V for NB-IoT end device with the data of sample No. 6.

Coefficient C	R-square (LoRa)	R-square (NB-IoT)
3.6	0.9974	0.9942
3.62	0.9973	0.9940
3.64	0.9964	0.9932
3.66	0.9948	0.9916
3.68	0.9920	0.9880
3.7	0.9875	0.9822

Table 4.5: Mean values of R-square values for LoRa and NB-IoT with different coefficient values C. The coefficient values C in $a \cdot \exp(-bt) + C$ ranges from 3.6 V to 3.7 V, with a step of 0.02 V.

4.1.2 Fitting by exponential function

For this part, we assume the curve from 4.2 V to 3.7 V is following the form $V = a \cdot e^{-bt} + C$. Based on the voltage data we collected, as we have presented in Figure 3.5 and Figure 3.6, there is a sharp transition when the voltage is below 3.65 V. To find the best coefficient C in the exponential function, we need to choose the constant that fitting the curve. The value of R-square shows how

set#	a	b	R-square
1	0.5448	0.0005542	0.997
2	0.5746	0.0005305	0.999
3	0.5463	0.0005293	0.999
4	0.5640	0.0005358	0.997
5	0.5023	0.0005407	0.995

Table 4.6: The exponential model fitting result of the voltage as a function of time for the LoRa end device with the data we collected during 5 trials.

set#	a	b	R-square
1	0.5216	0.001186	0.992
2	0.5136	0.001370	0.993
3	0.5526	0.001087	0.997
4	0.5528	0.001146	0.996
5	0.5454	0.001202	0.998
6	0.5229	0.001256	0.991

Table 4.7: The exponential model fitting result of the voltage as a function of time for the NB-IoT end device with the data we collected during 6 trials.

well the data fit the curve. Then we calculate the R-square values for different C between 3.6V and 3.7 V to find out the best constant for the exponential function. The R-square values are calculated by `cftool` in Matlab and the results are shown in Table 4.5. We can see when $C=3.6$, R-square values are closest to 1, which means the $C=3.6$ is the best coefficient for both cases. Then the exponential function is

$$V = a \cdot e^{-bt} + 3.6. \quad (4.1)$$

Based on our data, we can calculate the corresponding a and b , as shown in Table 4.6 and Table 4.7. We can see the R-square for every sample is close to 1, which means that the fitting shows good performance. To visualize the result, we use the same sample in Section 3.5.1. For LoRa part, we use sample No.5 in Table 4.6. For NB-IoT part, we use sample No.6 in Table 4.7. It makes no difference which sample is chosen since all the R-square values are similar. The results are shown in Figure 4.5 and Figure 4.6. We can see that most data points fit the curve, which means the exponential model has a good performance. We conclude that the exponential model also shows good fitting performance.

However, we could not find a way to use the coefficients we get from the exponential model to calculate the power consumption. The linear model is more direct for the calculation. In conclusion, we choose the linear model for future analysis.

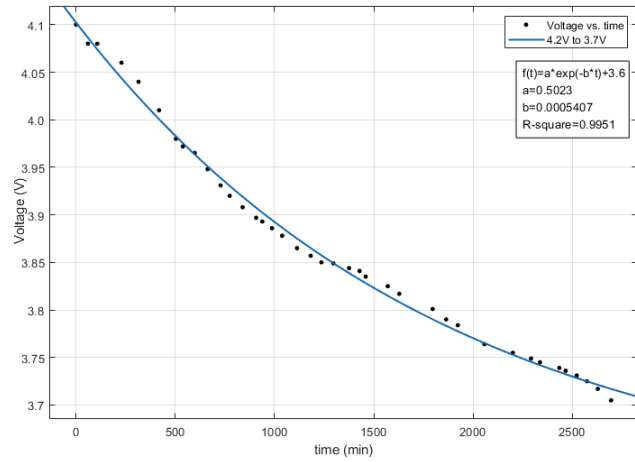


Figure 4.5: The fitting exponential function of the voltage for LoRa end device with the data of sample No 5.

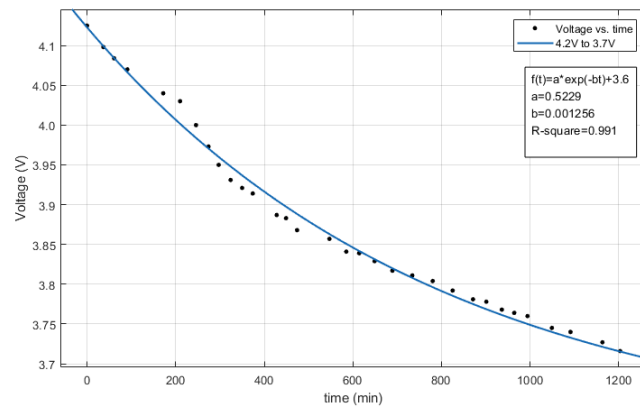


Figure 4.6: The fitting exponential function of the voltage for NB-IoT end device with the data of sample No 6.

		mean
LoRa Arduino board	4.2 V to 3.9 V	-2.2120e-04
	3.9 V to 3.7 V	-9.9184e-05
NB-IoT Arduino board	4.2 V to 3.9 V	-2.0055e-04
	3.9 V to 3.7 V	-1.8570e-04

Table 4.8: The mean values of the slope of the voltage transitions for Arduino boards without running codes

4.2 Comparison

From the previous section, we get the slope for the voltage transition. To compare the power consumption of two communication protocols, we need to exclude the power consumption of the Arduino board itself. In our experiments, we measured the voltage transitions of the Arduino boards without running codes. Applying the same linear model ($V_1(t) = p_1t + C_1$ for 4.2 V to 3.9 V and $V_2(t) = p_2t + C_2$ for 3.9 V to 3.7 V), we get the slope of voltage transition, as shown in Table 4.8.

To construct the power consumption model, we denote the transmission power of the RF unit by P_{trans} . In a time period, it takes t_{trans} for the end node to transmit a message. The rest of time is the idle period, which is denoted by t_{idle} . P_{idle} is the power consumption in the idle period. Then the average power of the node in this time period is

$$P_{\text{avg}} = \frac{P_{\text{trans}} \cdot t_{\text{trans}} + P_{\text{idle}} \cdot t_{\text{idle}}}{t_{\text{trans}} + t_{\text{idle}}}. \quad (4.2)$$

The total power consumption also contains the power consumption of the Arduino board, which is denoted by P_{board} . The total average power is

$$P_{\text{total}} = P_{\text{avg}} + P_{\text{board}}. \quad (4.3)$$

Then we can calculate the P_{board} and P_{total} separately:

$$\begin{aligned} E_{\text{battery}} &= P_{\text{board}} \cdot t_1, \\ E_{\text{battery}} &= P_{\text{total}} \cdot t_2, \end{aligned} \quad (4.4)$$

where t_1 is the time for running the Arduino board without running any codes from 4.2 V to 3.7 V and t_2 is the time for running the Arduino board when transmitting the data every 10 seconds. Combining Eq (4.3) and Eq (4.4), we can calculate the P_{avg} :

$$P_{\text{avg}} = \frac{E_{\text{battery}}}{t_2} - \frac{E_{\text{battery}}}{t_1}. \quad (4.5)$$

We calculate t_1 and t_2 as

$$t = \frac{\Delta V_1}{k_1} + \frac{\Delta V_2}{k_2} \quad (4.6)$$

$$= \frac{0.3}{k_1} + \frac{0.2}{k_2}, \quad (4.7)$$

where k_1 is the slope value for the linear function from 4.2 V to 3.9 V and k_2 is the slope value for the linear function from 3.9 V to 3.7 V. To get the value of t_1 and t_2 , we apply the slope value we got from Table 4.2, Table 4.4, and Table 4.8. According to [13], the energy consumption from 4.2 V to 3.7 V is around 80% of the battery capacity. Then $E_{battery}$ is the 80% energy of a 3.8 V 3000 mAh Li-Po battery, which is 32832 joules. Using these values, we can get P_{avg} .

For LoRa:

$$\begin{aligned} P_{avg, LoRa} &= \frac{E_{battery}}{t_2} - \frac{E_{battery}}{t_1} \\ &= 442.8\text{mW}. \end{aligned} \quad (4.8)$$

For NB-IoT,

$$\begin{aligned} P_{avg, NB-IoT} &= \frac{E_{battery}}{t_2} - \frac{E_{battery}}{t_1} \\ &= 607.7\text{mW}. \end{aligned} \quad (4.9)$$

(For NB-IoT, we used the data from 4.2 V to 3.7 V and the transmit power became 16.54 W which is a ridiculous result. We considered 3.9 V to 3.7 V is the steady area for analysis since the battery capacity decays with time and affects the behavior for 4.2 V to 3.9 V. According to [13], it is around 50% of the battery capacity, which is 20520 joules.)

With the P_{avg} , we can calculate the P_{trans} for LoRa and NB-IoT.

- LoRa:

The payload size is 50 Bytes. The ToA for SF7/125 kHz is 97.54 ms. Recall that time interval for the transmissions is 10 seconds. Thus, the idle time is $t_{interval} - t_{trans} = 9.902$ seconds. To calculate the transmit power, we assume the power consumption for idle period is the current consumption in sleep mode, as introduced in Table 3.2. The supply current in sleep mode is $1.4 \mu\text{A}$. Using Eq (4.2), we get $P_{trans, LoRa} = 453.5 \text{ mW}$.

- NB-IoT:

For the NB-IoT, the packet structure is complicated and the data rate is calculated through the experiment measurement.

To calculate the time for transmitting a packet in the experiments, we measured the total transmission time for 1000 packets. The average total time is 86 s, so the transmission time for 1 packet is 86 ms. Using Eq (4.2), we get $P_{trans, NB-IoT} = 2.686 \text{ W}$.

For the experiment data, we can see SF7/125 kHz has a lower power consumption of the transmit power and the average power. However, as introduced before, the SF7/125 kHz has the lowest power consumption at the expense of coverage. Also, the increasing payload size may change the result.

In the following section, we will discuss the performance of LoRa and NB-IoT by changing these parameters.

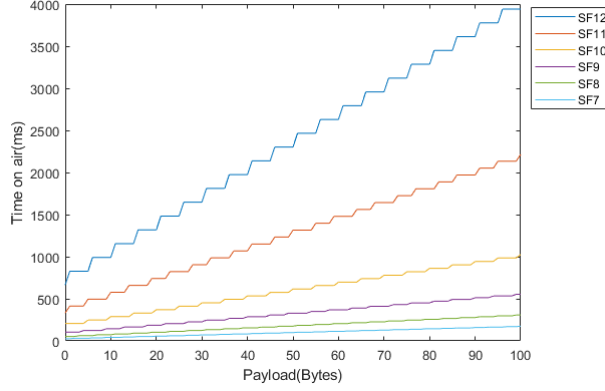


Figure 4.7: ToA vs payload size for different spreading factors. The payload size ranges from 0 to 100 Bytes.

4.3 Performance of LoRa with different spreading factors

Using Eq (2.3), Eq (2.4) and Eq (2.5), we can calculate the ToA for different spreading factor and bandwidth. Here we assume the bandwidth is 125 kHz. Then we have:

$$ToA = \frac{2^{SF}}{BW} \left(20.25 + \max \left(\text{ceil} \left[\frac{8PL - 4SF + 44 - 20IH}{4(SF - 2DE)} \right] (CR + 4), 0 \right) \right). \quad (4.10)$$

Note: $IH=1$ since explicit header is default on for LoRaWAN. Low data rate optimization is enabled for bandwidth 125kHz and Spreading factor ≥ 11 . Then we can plot ToA vs payload size for different spreading factors, as shown in Figure 4.7. The ToA increases when the spreading factor becomes larger and the gap is larger when the payload size keeps increasing. The larger the ToA, the larger the power consumption. In our experiment, we use spreading factor 7 to transmit data with 50 Bytes payload. The ToA equals to 2301.95 ms for $SF=12$ and equals to 97.536 ms for $SF=7$ when payload size=50 Bytes. If we choose spreading factor 12 to transmit the same data, the ToA will be about 22 times longer as compared to the ToA with spreading factor 7.

To check the power efficiency, we introduce the energy per useful bit:

$$E_{\text{bit}} = \frac{P_{\text{trans}} \cdot ToA}{8PL}, \quad (4.11)$$

where PL stands for the payload size, P_{trans} is the transmit power we got from the experiment. Then the the results of the energy consumption per useful bit with different total payload size are given in Figure 4.8. When the payload size is not big, the energy per useful bit is large due to the preamble and header length, and the influence of the spreading factor is greater. When the payload size increases to a certain level, the energy per useful bit becomes stable for every spreading factor.

We take the values when the payload size is 50 Bytes for comparing the

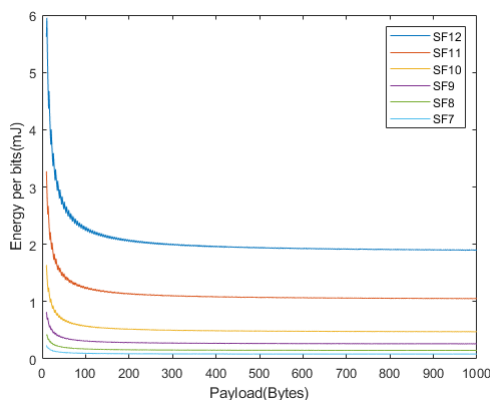


Figure 4.8: Energy per useful bit vs payload size for different spreading factors. The payload size ranges from 0 to 1000 Bytes.

Spreading factor	Energy per useful bit (mJ)
SF7	0.084
SF8	0.147
SF9	0.262
SF10	0.474
SF11	1.049
SF12	1.895

Table 4.9: Energy per useful bit for different spreading factors (Payload size=1000 Bytes)

energy per useful bit for different spreading factors. The results are shown in Table 4.9. The difference brought by spreading factors is huge when the transmit power and payload are the same. The biggest energy per useful bit (SF12) is 19.7 times the smallest one (SF7). However, larger spreading factors have a greater coverage with the same transmit power. According to [14], the receiver sensitivity is -136 dBm for SF12 and -123 dBm for SF7. The lower level of the value means the receiver sensitivity is better. This shows that the coverage of SF12 much better than SF7 given that the transmit power is the same. There is a trade-off between the coverage and power consumption.

Since the same transmit power will lead different coverage, we want to figure out whether the energy consumption will become smaller than SF7 if SF12 choose small transmit power. According to SX1276 specifications [14], we can find the power consumption with different transmit power, as shown in Table 4.10.

According to the data sheet, the experiment data for the transmit power may use the largest transmission power 20 dBm. To enable the same coverage level, we introduce the Maximum Coupling Loss (MCL), which is used to describe supported coverage. According to [15], the MCL is calculated as

$$\text{MCL} = \text{TX power} - \text{RF sensitivity} . \quad (4.12)$$

To ensure the same range with SF7 using 20 dBm, SF12 can use 7 dBm transmit

Transmission Power (dBm)	Power consumption (mW)
20	396
17	287
13	95.7
7	66

Table 4.10: SX1276 characteristics

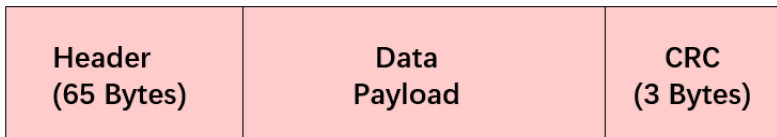


Figure 4.9: NPUSCH packet structure

power. Since we have the energy per useful bit using SF12 when the transmit power is 20 dBm, we can use the ratio of the power consumption in the data sheet to get the corresponding energy per useful bit using SF12 with 7 dBm transmit power. Then the new value of energy per useful bit using SF12 is $E_{\text{bit}} = 0.316$ mJ. It is still much larger than the one of SF7, but the gap is smaller.

From this part, we can see the spreading factor has great influence on the energy consumption. In NB-IoT uplink scheme, many parameters also have great impact on the energy consumption, as we will show in the next section.

4.4 Performance of NB-IoT for different subcarrier spacing

For NB-IoT uplink transmission scheme, the repetition times and the subcarrier spacing will affect the transmission time for the data. The increase of the transmission time makes the energy consumption larger. In this part, we will discuss the effect brought by these two parameters.

According to [25], the NPUSCH packet structure is shown in Figure 4.9. In the experiments, our payload length is 50 Bytes but we do not know the header length of the upper layer. To calculate transmission time, we assume the header length of the upper layer is L Bytes and the payload size is 50 Bytes. Then we need to calculate the total number of bits transmitted and find the corresponding transmission time. Using the relationship between the transmission time and header length L , we can find the approximate header length L based on our measured transmission time.

The maximum supported TBS is 1000 bits [8]. Assume $50+L$ Bytes are sent by $N+1$ packets, where N packets are 1000 bits long and the remaining packet is k bits long. Then it holds that $8(50 + L) = N \cdot 1000 + k$ bits. The header length and CRC for every packet is 544 bits [25]. Then the total block size is $N \cdot 1544 + (544 + k)$ bits. Using QPSK modulation and 1/3 code rate, we get the total number of transmitted symbols ($N \cdot 2316 + 816 + 1.5k$ symbols).

Number of subcarriers	Header length (Bytes)
12	420
6	185
3	68
1	N/A

Table 4.11: Calculated header length for different options

The measured transmission time is 86 ms for 50 Bytes payload. We were not clear which spacing the nodes uses, so we calculated the estimated payload size for every possible option. There are 4 options for 15 kHz spacing as described in Table 2.4.

Take the option of 12 subcarriers and RU 1 ms as an example, the calculation of the transmission time is shown as below:

For 15 kHz subcarrier spacing, there are 168 resource elements (12 subcarriers \times 7 \times 2 symbols) in one subframe. For each subframe, the NPUSCH format 2 occupies 14 resource elements and DMRS occupies 6 subcarriers. The available resource elements for each subframe is 148 [25]. Then we can calculate the number of subframes as

$$N_{\text{subframe}} = \frac{I_{\text{symbols}}}{N_{RE}}. \quad (4.13)$$

Then the number of subframes needed for uplink transmitting in NPUSCH is $(N \cdot 2316 + 816 + 1.5k)/148$. The duration of a single subframe is 1 ms. According to [26], 30% uplink resources are reserved for NPRACH. Then the total time for the transmission is calculated by following equation.

$$\begin{aligned} T_{\text{transmission}} &= T_{\text{subframe}} \cdot N_{\text{subframe}} \cdot T_{CTRL} \\ &= 1\text{ms} \cdot \frac{N \cdot 2316 + 816 + 1.5k}{148} \cdot \frac{1}{1 - 30\%} \\ &= \frac{N \cdot 2316 + 816 + 1.5k}{103.6} \text{ ms}, \end{aligned} \quad (4.14)$$

where T_{CTRL} is the overhead factor due to control information (NPRACH). Then the total transmission time is $((N \cdot 2316 + 816 + 1.5k)/103.6)$ ms.

Using the same method, we can calculate the corresponding header length for each option when the transmission time is 86 ms. Then we can find out the approximate header length for upper level in order to do further discussion.

The result is shown in Table 4.11. According to [27], the header length of higher layers is around 65 Bytes. Then We conclude that 68 Bytes is the appropriate value for our experiments. Then when we transmit useful bits L Bytes, the payload size is (68+L) Bytes.

According to [28], the subframe should be repeated 64 times to achieve the BLER 7% with the coverage of 164 dB MCL (Maximum coupling loss). The MCL is 144 dB when the subframe is not repeated. Then we plot the case of 1 repetition and 64 repetitions respectively. The result is shown in Figure 4.10. We can see that the transmission time increases when the payload size increases. More tones for transmission will lead to less transmission time. The transmission time and the related power consumption is increased a lot when the subframe is repeated for better coverage. There is a trade-off between the coverage and the power consumption.

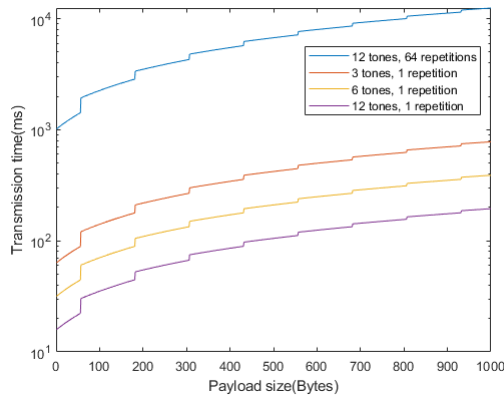


Figure 4.10: Transmission time vs payload size with 1 repetition and 64 repetitions. The cases of 1 repetition include 3 tones, 6 tones and 12 tones.

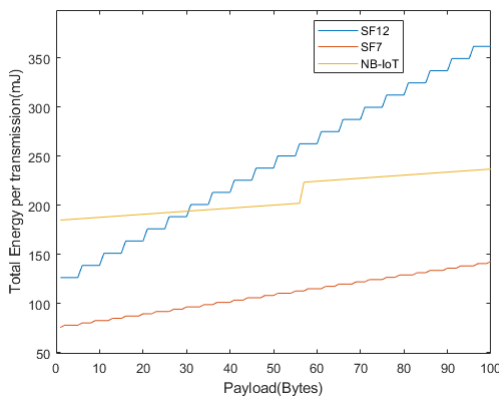


Figure 4.11: The energy per transmission as a function of payload size for SF7, SF12, and NB-IoT.

4.5 Battery lifetime comparison

For those LPWANs, the power consumption can be reduced at the expense of the coverage. We choose SF12 with transmit power 7 dBm and SF7 with 20 dBm for LoRa. We choose MCL=144 dB, 12 tone and 1 repetition for NB-IoT to compare the power consumption of two protocols in the similar level of coverage. The application of the LPWANs usually has long transmission interval. In this part, we assume the message is sent once an hour. Then we plot the energy consumption for every transmission and sleep period vs payload size. The result is shown in Figure 4.11.

In this scenario, NB-IoT has the higher energy consumption when the payload size is very small. With the increase of the payload size, the energy consumption of NB-IoT is smaller than SF12 but still larger than SF7.

For LPWAN applications, the payload size of 100 Bytes is a proper choice [27]. Here we calculate the estimated battery life for our devices in this scenario.

	Battery Life (Years)
LoRa (SF7)	32.7
LoRa (SF12)	12.9
NB-IoT	19.8

Table 4.12: Estimated battery lifetime.

We assume the battery capacity is 3000 mAh, which is the same as we used in the experiment. The power consumption of the sleep period is based on Table 3.2 and Table 3.4. Note: The maximum payload size of SF12 is 55 Bytes, so the message needed to be sent in two packets and the second packet needs to wait for a duty cycle. The total transmission time and idle time will not change, so it will not affect the power consumption.

The results show that LPWAN applications have long battery lifetime when we transmit message once an hour. LoRa with SF7 provides the longest estimated battery lifetime. NB-IoT with 12 tones and 1 repetition has lower power consumption than LoRa with SF12.

However, the resource blocks of the NB-IoT are shared by all devices and we assume no other traffic in this scenario. So, the actual energy consumption of the NB-IoT will be higher. In addition, 12 tones and 1 repetition for NB-IoT provides the least transmission time. This is the optimal situation and the NB-IoT cannot provide less power consumption than this case when the signal is very good and coverage is not a concern.

Chapter 5

Conclusion

In this thesis, the objective is to compare the energy consumption of LoRaWAN and NB-IoT based on the experimental data and calculation. We measured the power consumption of NB-IoT and LoRa by using Arduino boards and transmitting the data every 10 seconds. Based on these results, we calculate the estimated battery lifetime for different parameters when the transmission interval is one hour. According to the results, LoRa with lower spreading factors has lower power consumption. For the same transmission interval (1 message/hour) and coverage level (MCL=144 dB), the battery lifetime of LoRa with spreading factor 12 is 39.4% of the one of LoRa with spreading factor 7. Longer ToA for larger spreading factor contributes to higher power consumption even if the coverage level is the same.

For the same transmission interval and coverage level, the NB-IoT provides higher power consumption and shorter battery lifetime. The estimated battery lifetime of NB-IoT with 12 tones and 1 repetition is 60.6% of the one of LoRa with spreading factor 7. NB-IoT consumes more power because of the synchronization and OFDM modulation. On the other hand, NB-IoT provides low latency and higher data rate than LoRa. There is a trade-off between them if the latency is a critical issue for the applications.

There are some possible future directions to improve the results of the thesis and to make the comparison more thorough.

In our experiments, we only measured the transmission for LoRa with SF7 and NB-IoT with 1 repetition. Due to the time constraints, we did not measure the power consumption of LoRa with SF12 and NB-IoT with more repetitions. Otherwise, it requires least time interval to be 230 seconds for transmitting a message with 50 Bytes. The period will be enlarged too much. Instead of measuring them, we assumed there is no congestion issue and calculated the power consumption of those parameters to do further comparisons. Future experiment on LoRa with SF12 and NB-IoT with more repetitions can make the result more convincing. In addition, we did not use the exponential model for the calculation. The exponential model fits the performance of the battery, so it could lead to more accurate result. Future analysis based on the exponential fitting is preferred.

The NB-IoT radio module we used in the experiment only supports the protocol stack of 3GPP Release 13. According to [29], the enhancement enables the power consumption reduction in Release 15. The performance on NB-IoT could

be better if using newest devices. The experiment on devices which support Rel 14 and Rel 15 is preferred.

Bibliography

- [1] "IoT security - protecting the networked society," Ericsson.com, 18-Sep-2019. [Online]. Available: <https://www.ericsson.com/en/white-papers/iot-security-protecting-the-networked-society>.
- [2] "Internet of Things forecast - Ericsson Mobility Report," Ericsson.com, 18-Sep-2019. [Online]. Available: <https://www.ericsson.com/en/mobility-report/internet-of-things-forecast>.
- [3] L. Krupka, L. Vojtech and M. Neruda, "The issue of LPWAN technology coexistence in IoT environment," 2016 17th International Conference on Mechatronics - Mechatronika (ME), Prague, 2016, pp. 1-8.
- [4] Alliance, L. A technical overview of LoRa and LoRaWAN. White Paper, November, 2015.
- [5] N. Sornin (Semtech), A. Yegin (Actility), "LoRaWAN 1.1 Specification," LoRa Alliance, Oct. 2017.
- [6] Standardization of NB-IoT completed. [Online]. Available: <http://www.3gpp.org/news-events/3gpp-news/1785-NB-IoT-complete>.
- [7] Grant S. 3GPP Low Power Wide Area Technologies-GSMA White Paper[J]. gsma. com, 2016.
- [8] Schlien J, Raddino D. Narrowband internet of things whitepaper[J]. White Paper, Rohde&Schwarz, 2016: 1-42.
- [9] O. Khutsoane, B. Isong and A. M. Abu-Mahfouz, "IoT devices and applications based on LoRa/LoRaWAN," IECON 2017 - 43rd Annual Conference of the IEEE Industrial Electronics Society, Beijing, 2017, pp. 6107-6112. doi: 10.1109/IECON.2017.8217061
- [10] Alliance L R. LoRaWAN Regional Parameters v1. 0[J]. LoRa Alliance: Fremont, CA, USA, 2016.
- [11] Semtech, "AN1200.22 LoRa Modulation Basics." [Online]. Available: http://things4u.github.io/DeveloperGuide/LoRa%20documents/Semtech_LoRa_Modulation.pdf.
- [12] Bouguera T, Diouris J F, Chaillout J J, et al. Energy consumption model for sensor nodes based on LoRa and LoRaWAN[J]. Sensors, 2018, 18(7): 2104.

- [13] Everything About LiPo Battery for Racing Drones - Oscar Liang. [online] Available at: <https://oscarliang.com/lipo-battery-guide/>.
- [14] Semtech, LoRa SX1276/77/78/79 Datasheet, Rev. 6, 2019. [Online]. Available: <https://www.semtech.com/products/wireless-rf/lora-transceivers/sx1276>
- [15] "Coverage Analysis of LTE-M Category-M1." [Online]. Available: <https://altair-semi.com/wp-content/uploads/2017/02/Coverage-Analysis-of-LTE-CAT-M1-White-Paper.pdf>
- [16] Access E U T R. User Equipment (UE) radio transmission and reception[J]. 3GPP TS, 2010, 36: V10.
- [17] "Telia - Sweden - Wireless Frequency Bands and Device Compatibility," FrequencyCheck. [Online]. Available: <https://www.frequencycheck.com/carriers/telia-sweden>.
- [18] Wang Y P E, Lin X, Adhikary A, et al. A primer on 3GPP narrowband Internet of Things[J]. IEEE communications magazine, 2017, 55(3): 117-123.
- [19] Arduino MKR WAN 1300. [Online]. Available: <https://store.Arduino.cc/Arduino-mkr-wan-1300-lora-connectivity-1414>
- [20] Type ABZ, Order Number CMWX1ZZABZ. [Online]. Available: <https://wireless.murata.com/type-abz.html>
- [21] Atmel SAM D21E / SAM D21G / SAM D21J Data sheet. [Online]. Available: https://cdn.sparkfun.com/datasheets/Dev/Arduino/Boards/Atmel-42181-SAM-D21_Datasheet.pdf
- [22] Arduino MKR NB 1500. [Online]. Available: <https://store.Arduino.cc/Arduino-mkr-nb-1500-1413>
- [23] SARA-R4 series LTE Cat M1/NB1 and EGPRS modules Data sheet. [Online]. Available: https://www.u-blox.com/sites/default/files/SARA-R4_DataSheet_%28UBX-16024152%29.pdf
- [24] "Data Rate and Spreading Factor," Exploratory Engineering: Data Rate and Spreading Factor. [Online]. Available: https://docs.exploratory.engineering/lora/dr_sf/.
- [25] Malik H, Pervaiz H, Alam M M, et al. Radio resource management scheme in NB-IoT systems[J]. IEEE Access, 2018, 6: 15051-15064.
- [26] NB-IoT-Initial Analysis of PRACH Capacity, document R1-157199, 3GPP, 2015.
- [27] Ericsson. Massive IoT in the city - Mobility Report. [online] Available at: <https://www.ericsson.com/en/mobility-report/massive-iot-in-the-city>.
- [28] A. Adhikary, X. Lin and Y. -. E. Wang, "Performance Evaluation of NB-IoT Coverage," 2016 IEEE 84th Vehicular Technology Conference (VTC-Fall), Montreal, QC, 2016, pp. 1-5. doi: 10.1109/VTCFall.2016.7881160

- [29] Ratasuk R, Mangalvedhe N, Xiong Z, et al. Enhancements of narrowband IoT in 3GPP Rel-14 and Rel-15[C]//2017 IEEE Conference on Standards for Communications and Networking (CSCN). IEEE, 2017: 60-65.

